scientific reports

Check for updates

OPEN

Hot melt extruded Kyungohkgo attenuates skeletal muscle atrophy by downregulating the FOXO3a/MuRF-1/atrogin-1 axis

Young Mi Seok[1,7], Bo-Ram Jin[2,7], Tae-Young Gil[2], Suji Ryu[3], Chan-Yeong Ju[4], Yoonah Jeong[1], Jinyoung Son[1], Man Sop Shim[5], Hyo Jung Kim[1], Hyo-Jin An[2,4]✉, Jong-Suep Baek[3,5]✉ & Yun-Yeop Cha[6]✉

Skeletal muscle atrophy is a common and debilitating consequence of chronic diseases and aging, yet effective treatment alternatives remain limited. Kyungohkgo (KOG), a traditional oriental medicine, has been shown to have potential therapeutic benefits for muscle health, but its therapeutic efficacy is restricted caused by poor bioavailability. This study aimed to enhance both the bioavailability and efficacy of KOG by applying hot-melt extrusion (HME) processing, creating a modified formulation to evaluate its effectiveness in treating skeletal muscle atrophy. Network pharmacology analysis was conducted to illustrate the relationships between the traditional medicine KOG and sarcopenia. Both in vivo and in vitro models of skeletal muscle atrophy were employed to compare the effects of conventional KOG and HME-processed KOG (HOG3). HME processing yielded an optimized formulation, HOG3, characterized by nanoscale particle size and a marked increase in minor ginsenoside content. In this study, HOG3 showed significantly higher ginsenoside levels than KOG, with Rg3, compound K, and Rh2 increasing approximately 19-, 78-, and 18-fold, respectively. In cellular and animal models, HOG3 outperformed KOG in preserving muscle mass, reducing muscle degradation markers, and decreasing collagen deposition. HOG3 administration was associated with decreased expression level of FOXO3a, MuRF-1, and atrogin-1. Overall, these findings show that HOG3 indicates enhanced protective effects against skeletal muscle atrophy and is associated with modulation of downstream molecular markers related to muscle degradation.

Keywords Dexamethasone, Ginsenoside, Hot-melt extrusion, Kyungohkgo, Skeletal muscle atrophy

Abbreviations

AA	Ascorbic Acid
ALP	Alkaline Phosphatase
ChIP	Chromatin Immunoprecipitation
Dexa	Dexamethasone
ELS	Electrophoretic Laser Scattering
FOXO	Forkhead Box O
FRE	FOXO3a-Response Element
GC	Glucocorticoid
GRE	GC-Response Element
GR	Glucocorticoid Receptor

[1]Industrial Growth Support Team, Department of Industry Promotion, National Institute for Korean Medicine Development, Gyeongsan 38540, Republic of Korea. [2]College of Pharmacy and Institute of Integrated Pharmaceutical Sciences, Kyung Hee University, Seoul 02447, Republic of Korea. [3]Department of Bio-Health Convergence, Kangwon National University, Chuncheon 24341, Republic of Korea. [4]Department of Biomedical and Pharmaceutical Sciences, Graduate School, Kyung Hee University, Seoul 02447, Republic of Korea. [5]BeNatureBioLab, Chuncheon 24206, Republic of Korea. [6]Department of Rehabilitative Medicine of Korean Medicine and Neuropsychiatry, College of Korean Medicine, Sangji University, Gangwon-do 26339, Republic of Korea. [7]Young Mi Seok, Bo-Ram Jin and Tae-Young Gil have contributed equally to this work. ✉email: hjan@khu.ac.kr; jsbaek@kangwon.ac.kr; omdcha@sangji.ac.kr

H&E	Hematoxylin and Eosin
HME	Hot-Melt Extrusion
HOG3	HME-Processed Kyungohkgo
KOG	Kyungohkgo
MuRF-1	Muscle RING Finger Protein-1
qRT-PCR	Quantitative Real-Time Polymerase Chain Reaction
SEM	Standard Error of the Mean
TSS	Transcription Start Site
UA	Ursolic Acid

Skeletal muscle is the largest metabolic organ in the human body, accounting for 40–50% of total body weight, and serving as the primary protein reservoir, containing 50–75% of the body's total protein content[1]. Skeletal muscle mass is an important determinant of strength, endurance, and overall physical ability. However, factors including nutritional deficiencies, muscle loss, aging, and physical inactivity can cause skeletal muscle atrophy, which is marked by a reduction in both the size and number of muscle fibers[2].

Sarcopenia refers to the age-associated decline in muscle mass, strength, and physical performance. Its prevalence ranges from approximately 25% at 70 years of age to 40% at 80 years, with muscle loss progressing at a rate of about 1–2% per year after the age of 50[3]. While sarcopenia is typically associated with aging, a comparable condition is also observed in younger individuals with chronic illnesses[4]. A 2019 analysis in the United States estimated the annual hospitalization cost related to sarcopenia at about USD 40.4 billion, highlighting a significant economic burden on the healthcare system[5]. Furthermore, a systematic review of 14 studies reported that, despite several confounding factors, patients with sarcopenia have higher medical costs[6]. Sarcopenia is also considered to increase the risk of functional impairment and mortality in older adults. In recent years, the need for treatment-related research has been emphasized due to the rapid expansion of the aging population and substantial increases of healthcare expenditures[7].

Prolonged exposure to elevated levels of glucocorticoids (GCs) is a key contributor to skeletal muscle atrophy, known as steroid-induced myopathy[8]. Owing to their immunosuppressive and anti-inflammatory properties, both endogenous and synthetic GCs — such as dexamethasone (Dexa), prednisolone, and budesonide — are extensively utilized to manage chronic inflammatory conditions, including chronic obstructive pulmonary disease, inflammatory bowel disease, and rheumatoid arthritis[9]. However, sustained administration of high-dose GCs can lead to steroid-induced myopathy in approximately 10% of patients, with a higher incidence in elderly populations[10]. Muscle atrophy may develop within 2–3 weeks in patients who take 16 mg of Dexa daily[11].

Although the precise mechanism underlying GC remains incompletely defined, it has been suggested that their cellular actions are primarily mediated through binding to intracellular glucocorticoid receptor (GR) a member of the steroid hormone receptor subfamily. Especially, Dexa exhibits a 20-30-fold higher binding affinity for GR than cortisol, the principal endogenous GC[12], implying a markedly greater propensity to provoke muscle atrophy as an adverse effect. In skeletal muscles, GC-GR signaling mainly plays as a central regulator of protein metabolism via transcriptional control[13]. Forkhead box O (FOXO) transcription factors—including FOXO1, FOXO3a, and FOXO4 — are involved in orchestrating the gene expression program that drive skeletal muscle atrophy[14]. Activation of FOXO proteins robustly induce the activation of E3 ubiquitin ligases, such as muscle RING finger 1 (MuRF-1; TRIM63) and muscle specific F-box protein (atrogin-1; FBXO32), thereby accelerating proteasomal degradation[15]. Despite substantial advances in elucidating these molecular pathways, effective therapeutic strategies to counteract skeletal muscle atrophy remains strikingly limited.

Against this backdrop, multi-herbal prescriptions have emerged as a compelling therapeutic paradigm for modulating skeletal muscle homeostasis. Kyungohkgo (KOG; Qiong-yu-gao in Chinese; Kei-gyoku-kou in Japanese), a traditional multi-herbal medicine widely used in East Asia, comprises four components: root of *Rehmannia glutinosa* Libosch, root of *Panax ginseng* C. A. Meyer, *Poria cocos* Wolf, and refined honey. Historically, KOG has been utilized to boost physical vitality and to mitigate age-related conditions such as generalized weakness, immune dysfunction or testicular impairment[16]. Accumulating evidence indicates that KOG exerts anti-inflammatory, anti-oxidant, and anti-fatigue activities[17], that are largely attributed to its phytochemical composition—particularly *P. ginseng*-derived ginsenosides, which have attracted growing attention as candidate therapeutics for sarcopenia[50]. Nevertheless, the clinical translation of ginsenosides has been hampered by their poor aqueous solubility and limited membrane permeability[51]. Therefore hot-melt extrusion (HME) technique applied to the KOG to address these pharmacokinetic constrains and unlock the full therapeutic potential of ginsenosides. HME is an established manufacturing process in the food and pharmaceutical industries, designed to enhance bioavailability by improving the dissolution, stability, and effective concentration of active compounds. Through physical modifications—such as particle size reduction, alteration of crystalline structure, and formation of solid dispersions—HME substantially improve solubility[18]. Particularly, this solvent-free process minimizes the risk of residual solvent toxicity and offers an environmentally sustainable alternative to conventional formulation strategies. Given that many bioactive constituents in herbal medicines exist in polymeric or glycosidic forms with inherently poor absorption, HME shows a rational and innovative approaching suggestion to overcoming these intrinsic limitations. In the context, diverse drug-delivery strategies have already been explored to develop the bioavailability of ginsenoside, the major active component from *P. ginseng*[52].

Given their documented potential to alleviate fatigue or stress-related conditions[53], we evaluated the therapeutic efficacy of HME-processed formulation of KOG. Therefore, we hypothesized that both KOG and HME-proceed KOG (HOG3) may attenuate skeletal muscle atrophy by modulating the expression of FOXO3a-associated atrophy markers, including MuRF-1 and atrogin-1. To figure out this hypothesis, we established

a Dexa-stimulated L6 cell model and a Dexa-induced skeletal muscle atrophy animal model, enabling a comprehensive evaluation of the anti-atrophic potential of KOG and HOG3.

Materials and methods

Network pharmacology analysis of KOG in muscle atrophy

Using databases such as SwissTargetPrediction (http://www.swisstargetprediction.ch/), CTD (https://ctdbase.org/) (restricted to Homo sapiens); all predicted proteins were mapped to official UniProt gene symbols and deduplicated. The GeneCards (https://www.genecards.org/) databases were searched using "muscle atrophy" as the keyword to obtain muscle-related target: FBXO32 (atrogin-1), TRIM63 (MuRF-1), or FOXO3. Afterward, the common targets for KOG and muscle atrophy were pinpointed, leading to the construction of "Drug-Compounds-Targets" and protein–protein interaction (PPI) network of these core targets was constructed via STRING (https://string-db.org/) using a minimum interaction score of 0.4 and visualized in Cytoscape v3.10.3. All potential therapeutic targets were subjected to Gene Ontology (GO) and Kyoto Encyclopedia of Genes and Genomes (KEGG) pathway enrichment analysis via the DAVID database (https://david.ncifcrf.gov/) to identify the related pathways and related GO terms, including those in the biological process (BP), molecular function (MF), and cellular component (CC) categories. The pathways and GO terms with applicable thresholds of $p < 0.05$ were considered significant and were retained. Additionally, Bioinformatics (http://www.bioinformatics.com.cn/) was used to visualize the GO and KEGG enrichment analysis results in a bubble plot of GO categories and bar graph of signaling pathways[19]. The network of active targets–signaling pathways–Disease was visualized using cytoscape v.3.10.3 software.

Preparation of KOG and HOG3

Roots of *Rehmannia glutinosa* Libosch, roots of *Panax ginseng* C. A. Meyer, *Poria cocos* Wolf, and refined honey were purchased from a traditional market located in Gangwon-do. To prepare KOG, the aforementioned ingredients were washed, cut into 3–5 mm sizes, dried, and blended 960 g of *Rehmannia glutinosa* Libosch, 90 g of *Panax ginseng* C. A. Meyer, 180 g of *Poria cocos* Wolf, and 640 g of refined honey. HOG3 was mixed according to the composition shown in Table 1. It was processed through a twin-screw extruder (STS-25HS) operating at 100 ℃ with a pressure of 35 bar and a screw speed of 50 rpm. Prepared KOG and HOG3 were extracted under reflux for 3 h using 10 times the weight of distilled water. The extract was purified using filter paper, evaporated at 40 ℃ using a rotary evaporator, and dried to obtain a powdered extract using a freeze dryer. Lyophilized KOG and HOG3 samples were then stored at 4 °C for subsequent experiments.

Determination of ginsenoside contents

To determine ginsenoside contents in KOG and HOG3, HPLC analysis was performed under the following condition. First, 1 g of KOG or HOG3 was added to 5 ml of 70% ethanol each, shaken, and subjected to ultrasonic extraction at 40 ℃ for 1 h. The extract was filtered using a 0.50 μm syringe filter before analysis. The HPLC system consisted of a Shimadzu LC-20AT HPLC system and a UV detector. A poroshell 120 SB-C18 column (3.0 × 50 mm, 2.7 μm) was used for compound analysis. The mobile phase was composed of acetonitrile (A) and water in 0.4% formic acid (B) at a flow rate of 1.0 ml/min. Gradient elution method was used according to the following schedule: 0–35 min: 95 to 65% (B), 35–40 min: 65 to 20% (B), 40–80 min: 20% (B).

Characterization of KOG and HOG3

The particle size was determined using an Electrophoretic Laser Scattering (ELS) analyzer (ELS-Z2; Otsuka Electronics, Osaka, Japan). Each sample was loaded onto a copper grid and air dried to observe the size and morphology using a Transmission Electron Microscopy (TEM, JEOL JEM-2010 F).

Cell culture

L6 rat myoblasts were obtained from the American Type Culture Collection (ATCC; Manassas, VA, USA, CRL-1458). These cells were maintained in Dulbecco's Modified Eagle's Medium (DMEM) enriched with 10% fetal bovine serum, along with 50 μg/ml of penicillin and streptomycin, at 37℃ in a humidified incubator containing 5% CO_2. To induce myogenic differentiation, L6 myoblasts at 90% confluency were transferred to a differentiation medium. The growth medium was substituted with DMEM supplemented with 2% horse serum, 50 μg/ml of penicillin, and streptomycin. The medium was refreshed every other day until day 7.

Quantitative real-time PCR (qRT-PCR)

L6 cells and muscles were homogenized in ice. Total RNA was extracted using a TRIzol Reagent (Invitrogen; Carlsbad, CA, USA) in accordance with the manufacturer's recommendations. The oligonucleotide primers designed from the rat genome for MuRF-1 were GCCATCCTGGACGAGAAGAAG (forward) and AGCGGCT

	HOG 1	HOG 2	HOG 3
KOG	100	98	90
Ascorbyl palmitate	0	2	2
Ascorbic acid	0	0	8
Total (%)	100	100	100

Table 1. Composition (%) of hot-melt extrusion (HME)-processed KOG (HOG).

TGGCACTCAAG (reverse), for atrogin-1 were GCAGAGAGTCGGCAAGTC (forward) and CAGGTCGGTG ATCGTGAG (reverse), for FOXO3a were CGGCTCACTTTGTCCCAGAT (forward) and TCTTGCCAGTCC CTTCGTTC (reverse), for Follistatin were CAGTGCAGCGCTGGAAAGAAAT (forward) and TGCGTTGCG GTAATTCACTTAC (reverse).

Western blot analysis

L6 cells were lysed in RIPA buffer supplemented with a 1× protease inhibitor cocktail. For western blotting, protein-equivalent samples (determined using the Bradford assay) were separated by electrophoresis on SDS-polyacrylamide gels and subsequently transferred onto nitrocellulose membranes. The membranes were then blocked with 5% skim milk in TBS (25 mmol/L Tris base and 150 mmol/L NaCl) for 2 h at room temperature, followed by overnight incubation at 4 °C with 1.0 μg/mL of each primary antibody. Antibodies targeting MuRF-1(Cat. No. ab183094, ab77577) and FOXO3a (Cat. No. ab12162) were sourced from Abcam (Cambridge, UK), while those for β-actin (sc-47778) were acquired from Santa Cruz Biotechnology (Santa Cruz, CA, USA). After three washes (10 min each) with Tris-buffered saline containing Tween 20 (TBST), the membranes were incubated with a secondary antibody (diluted 1:2000) at room temperature for 1 h. Following three additional washes with TBST (10 min each), the target proteins were visualized using ECL Plus detection reagents (Amersham; Pittsburgh, PA, USA). Protein expression levels were quantified via optical densitometry and analyzed using ImageJ software.

Chromatin immunoprecipitation (ChIP) assay

L6 cells were subjected to ChIP analysis as described previously[20]. The cells ($1*10^6$ cells/mL) were plated in 100 mm dishes and fixed with 1% formaldehyde, followed by washing with ice-cold PBS. After homogenization, samples were lysed in SDS buffer on ice for 30 min and sonicated for 15 cycles (10 s on and 50 s off at 100 amplitude). The lysates were precleared with protein G agarose for 2 h, then incubated overnight at 4 °C with primary antibodies. Protein G beads were added again and rotated for 1 h. Beads were sequentially washed with low-salt, high-salt, LiCl, and TE buffers. Chromatin-antibody complexes were eluted using 1% SDS/0.1 M $NaHCO_3$, and crosslinks were reversed at 65 °C for 5 h after adjusting NaCl to 0.2 M. Proteins were digested with proteinase K (45 °C, 2 h) and DNA was purified using spin columns. Antibodies used were FOXO3a (ab12162) and RNA polymerase II (ab5095, Abcam), and GR (sc8992X, Santa cruz). Promotor enrichment was quantified by real-time PCR in triplicate using the following cycling conditions: 50 °C for 2 min, 95 °C for 10 min, then 40 cycles of 95 °C for 15 s and 60 °C for 1 min. Relative enrichment was calculated using calculation the values of the change in cycle threshold (ΔCt) by normalizing the average Ct value to its control B 'input' Ct value and then calculating $2^{-\Delta\Delta Ct}$ values by comparing between groups[20]. The primers designed from the rat genome for MuRF-1 were CTTCTTCATGAAACTAGGGTACCTG (forward) and GAGCATTCCGAAGCCAAG (reverse), for atrogin-1 were AGGCTCTTCCGGCAACAAA (forward) and CGCAGTATTTATCCCGGGC (reverse), for FOXO3a GRE1 were GGACTGGGGATACTTGGAGC (forward) and GAACGAAAAGCGCTGCCTC (reverse), for FOXO3a GRE2 were GCGTGGCTTGACGAGGAA (forward) and CGAAACTCCGGCCTCCA G (reverse).

Animals

This study is reported in accordance with the ARRIVE guidelines (https://arriveguidelines.org). Animal studies were carried out in compliance with the National Institutes of Health Guidelines for the Care and Use of Laboratory Animals and were approved by the Animal Experimental Committee of the National Institute for Korean Medicine Development (NIKOM-2022-13). All possible measures were taken to reduce both the number of animals used and any potential distress. Seven-week-old male Sprague-Dawley (SD) rats were obtained from Koatech (Pyeongtaek, Korea) and housed in a controlled environment (23 ± 1℃ with 40–60% relative humidity) under a 12-hour light/dark cycle. They were provided unrestricted access to water and a standard laboratory diet. After a one-week adaptation period, dexamethasone (600 μg/kg body weight) or normal saline was administered via intraperitoneal injection once daily for five consecutive days. KOG (100, 200 mg/kg body weight) or HOG3 (100, 200 mg/kg body weight) was orally given once daily for three weeks. At the conclusion of the experiment, the rats were euthanized following 8 h of fasting before intraperitoneal injection of sodium pentobarbital (50 mg/kg body weight), and the soleus and gastrocnemius muscles were promptly harvested. These muscle tissues were then sectioned for further biological analysis and histological evaluation.

Histological analysis

Soleus and gastrocnemius muscles were fixed overnight in a 10% formalin solution, followed by dehydration and paraffin embedding using a standard procedure. The paraffin-embedded tissues were then sliced into 3-μm-thick sections. These sections were stained with hematoxylin and eosin (H&E) as well as Masson's trichrome. The prepared slides were observed under a light microscope, and expression levels were measured using optical densitometry and analyzed with ImageJ software.

Alkaline phosphatase (ALP) activity assessment

Blood samples were obtained from all test animals, and the serum was subsequently isolated. ALP activity was measured using a commercially available colorimetric assay kit, following the protocol provided by the manufacturer.

Statistical analysis

Data are presented as mean ± SEM. Statistical comparisons were conducted using Student's t-test, with significance defined at $p < 0.05$. All statistical analyses were carried out using SigmaPlot 10.0 software (Systat

Software Inc., Erkrath, Germany). The results from the HPLC experiment were evaluated using the SAS program (version 9.2; SAS Institute Inc., Cary, NC, USA). Differences between samples were assessed using Duncan's Multiple Range Test (DMRT) at a 5% significance level ($p < 0.05$).

Results

Identification of ingredients-targets-muscle atrophy network

The authors applied pharmacological network analysis to find the mitigatable sarcopenia targets of KOG active ingredients. Protein-protein interaction (PPI) network of target genes derived from *P. ginseng*, *P. cocos*, *R. glutinosa*, and *Mel* (honey) in Fig. 1a. It was consisted of active compounds of KOG, the predicted targets and known muscle atrophy-related genes, resulting in a deeply interconnected system. Major hub nodes like FBXO32, TRIM63, and FOXO3, were determined as central regulators, each presenting extensive interactions with multiple signaling molecules including TNF, STAT3, MAPK1, or IL-6. In addition, pathway enrichment analysis emphasized that the overlapping targets were mainly concentrated in the FOXO signaling pathway (Fig. 1b). Expansion of the network to biological processes demonstrated relations to muscle degeneration, apoptosis, and insulin resistance, while also linking to protected processes like muscle strength regulation (Fig. 1c). GO enrichment analysis was conducted to further characterize the functional role of those targets in Fig. 1d. And, KEGG enrichment was performed based on common targets to clarify the potential molecular pathways of KOG active ingredients in regulating muscle atrophy (Fig. 1e). In short, these results suggest that the KOG ingredients mitigated the muscle atrophy progression likely though the FOXO signaling pathway.

Determination of ginsenoside contents

In this work, HOGs were fabricated through the HME technique. HOGs consisted of proper polymer forming nano-sized particles. Contents of minor ginsenosides can be enhanced. Minor ginsenosides are known to exhibit significant therapeutic effects and improved bioavailability in comparison with major ginsenosides[21]. To compare minor ginsenosides such as Rg3, Compound K, and Rh2 in KOG and various HOG formulations (HOG1, HOG2 and HOG3), HPLC analysis was performed. Contents of minor ginsenosides such as Rg3, compound K, and Rh2 in all samples were compared (Fig. 2a). These three compounds were not detected in KOG. However, they were detected in HOG3. Ginsenoside content might be affected by additives in HOG3. Among all samples, HOG3 had the highest ginsenoside content. Its Rg3, compound K, and Rh2 contents were increased by about 19-, 78-, and 18-folds compared to that of HOG1, respectively. Since HOG3 exhibited the highest minor ginsenoside contents, it was selected for further studies.

Characterization of KOG and HOG3

TEM images of KOG and HOG3 were compared, revealing that the HME process successfully prevented aggregation of KOG with formation of a monodispersed colloidal dispersion (Fig. 2b and c). Results of ELS analysis indicated that the particle size was 1702.6 ± 305.7 nm for KOG and 177.23 ± 25.1 nm for HOG3 (Fig. 2d and e). In addition, it was revealed that HOG3 exhibited spherical nanoparticles. Upon HME process, excipients used were properly mixed with raw materials, followed by generation of tiny particles. The high shear force generated by twin screws of the HME process is known to effectively reduce the particle size from micro scale to nano scale[22].

HOG3 treatment enhances myoblast differentiation in Dexa-exposed L6 cells

To determine cytotoxicities of KOG and HOG3, cell viability was examined using L6 cells, myoblast cells isolated from rat skeletal muscles. Exposure to KOG at concentrations ranging from 40 to 600 μg/ml showed no impact on L6 cell viability (Fig. 3a). Similarly, treatment with HOG3 (40–600 μg/ml) did not affect L6 cell viability (Fig. 3b). Next, L6 myoblast cells were differentiated for one week. Differentiated L6 cells formed myotubes. The differentiated myotubes were exposed to Dexa (20 nmol/L) for 12 h, followed by treatment with KOG or HOG3 (100, 300, and 600 μg/ml) for 8 h. Stimulation with Dexa induced muscular dystrophy in L6 myotubes. In contrast, treated with KOG or HOG3 notably expanded sizes of myotubes (Fig. 3c). Based on microscopic images of representative samples for each group, we measured diameters of myotubes. In the Dexa-treated group, diameters of myotubes were significantly decreased in comparison with those of the Control group. Conversely, treatment with HOG3 at 300–600 μg/ml significantly restored sizes of myotubes (Fig. 3d).

Treatment with KOG or HOG3 reduces the expression of MuRF-1, atrogin-1, and FOXO3a in Dexa-induced L6 cells

To examine the effects of KOG and HOG3 on the expression of key atrophy-related genes, we investigated the involvement of MuRF-1 and atrogin-1. Stimulation with Dexa induced significant increases of MuRF-1 and atrogin-1 mRNA expression levels in L6 cells. However, KOG at 600 μg/ml and HOG3 significantly downregulated MuRF-1 mRNA levels (Fig. 4a and b). HOG3 at 600 μg/ml only significantly suppressed the mRNA level of atrogin-1. Stimulation with Dexa also significantly increased MuRF-1 protein expression in L6 cells. In this study, we used ursolic acid (U.A.) as positive control. Treatment with KOG at 600 μg/ml and HOG3 at 300–600 μg/ml significantly inhibited the upregulation of MuRF-1 protein expression induced by Dexa (Fig. 4c and d). Dexa stimulation significantly increased both mRNA and protein expression levels of FOXO3a, whereas treatment with HOG3 significantly suppressed FOXO3a mRNA and protein expression levels, showing a better effect than the positive control (Fig. 4d and g).

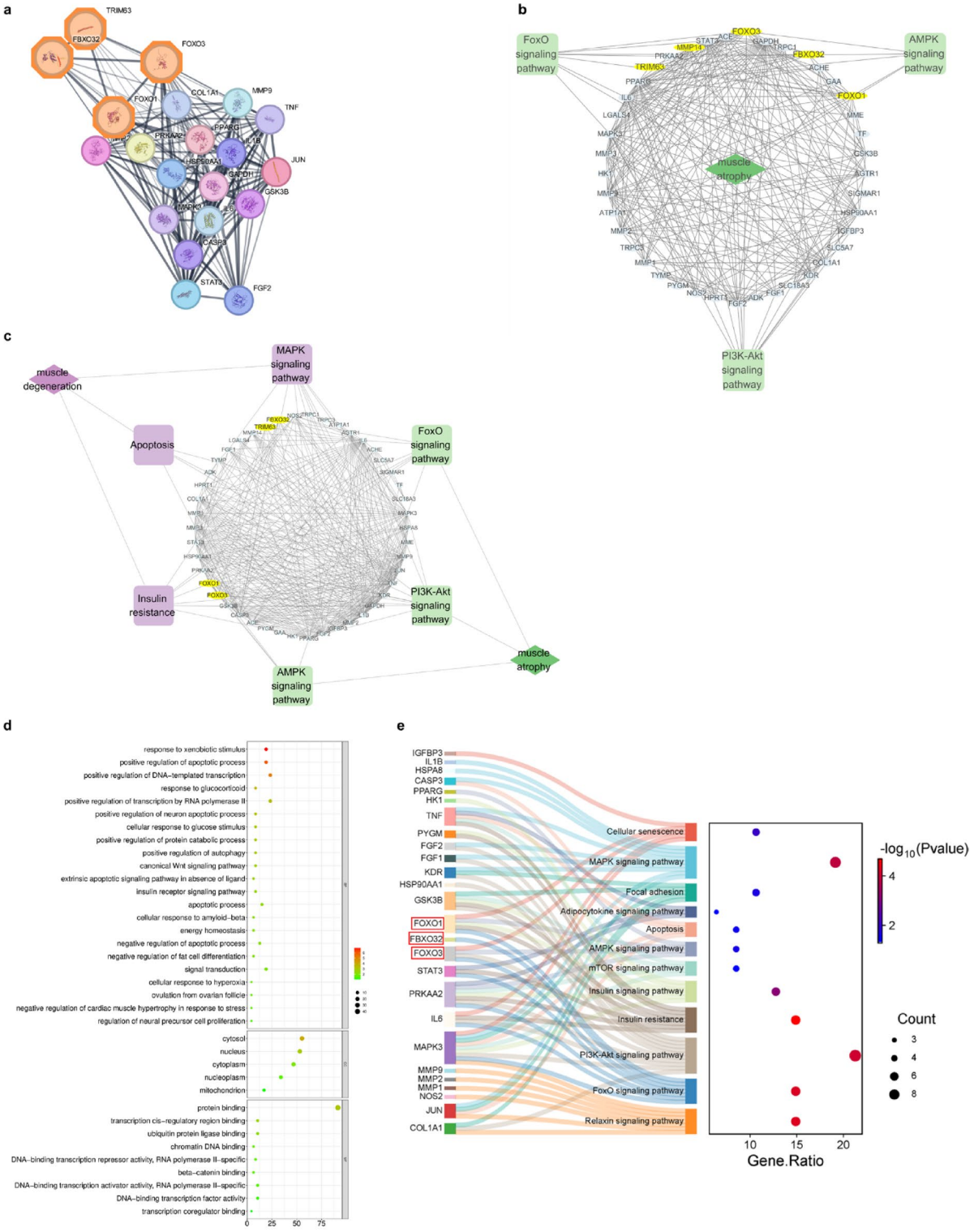

Fig. 1. Network pharmacology and enrichment analyses illustrating the potential mechanisms of KOG modulating muscle atrophy (**a**) PPI network of target genes derived from KOG ingredients and their compounds (**B**) Network centered on muscle atrophy depicting the associations between related genes and enriched signaling pathways, including FOXO (**c**) Integrated network connecting compound-target genes to make muscle-related diseases and enriched KEGG signaling pathways (**d**) GO enrichment analysis of target genes categorized into BP, CC, and MF (**e**) KEGG pathways enrichment and gene-pathway interaction shown via Sankey and dot plots.

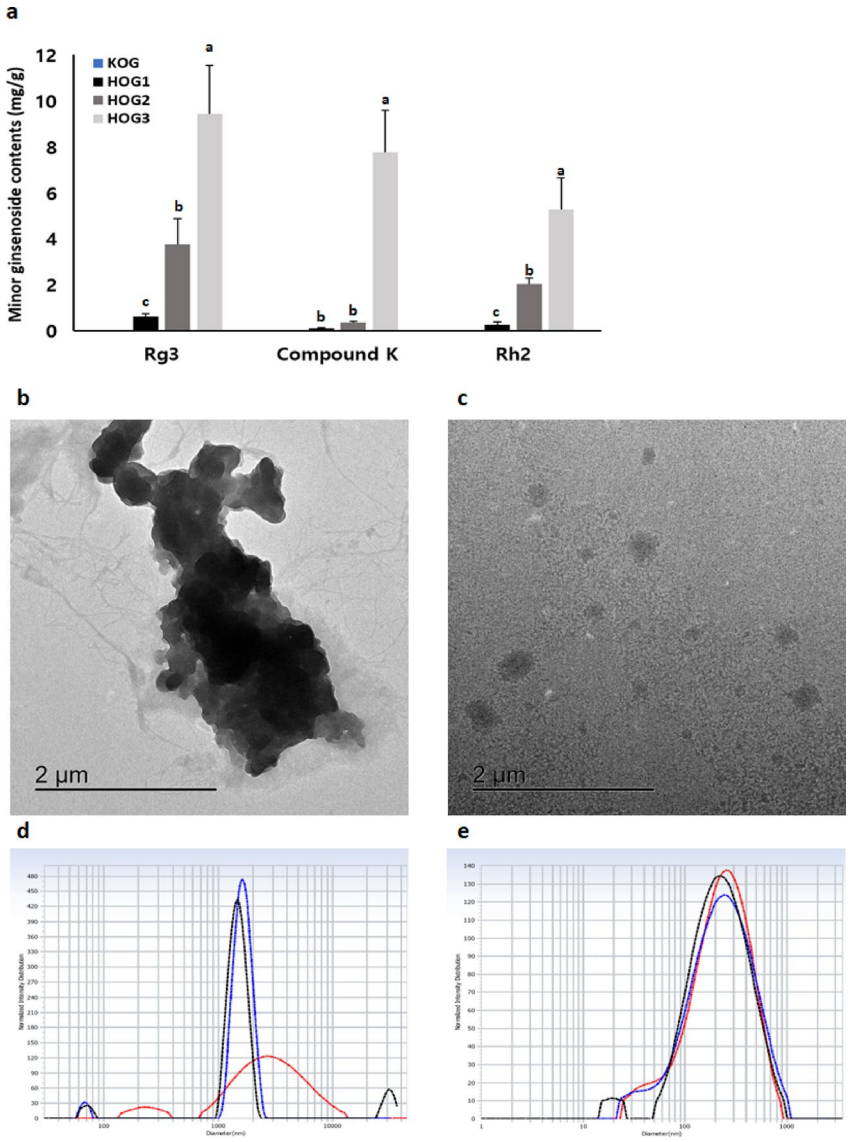

Fig. 2. Ginsenoside Rg3, compound K, and ginsenoside Rh2 contents in KOG and HOG3 ($n = 3$, Mean ± SD). Kyungohkgo, KOG; HME-processed KOG, HOG. (**a**) Comparison on minor ginsenoside contents of KOG, HOGs: HOG1, HOG2, HOG3. (**b**, **c**) Transmission electron microscopy (TEM) images of (b) KOG and (c) HOG3 and (**d**, **e**) particle distribution of (d) KOG and (e) HOG3.

Treatment with HOG3 reduces Dexa-induced promoter occupancy of FOXO3a, MuRF-1, and atrogin-1

To examine whether KOG and HOG3 affect Dexa-induced transcriptional regulation of FOXO3a, MuRF-1, and atrogin-1, ChIP assays were conducted in L6 cells. The binding of GR or RNA polymerase II (Pol II) to two GC-response elements (GRE1 and GRE2) within the rat rat FOXO3a promoter was analyzed. ChIP scanning figured out consensus GRE1 and GRE2 sequences located at − 1871/− 1861 and − 1026/− 1015 from the transcription start site (TSS), respectively (Fig. 5a and b, upper). Stimulation with Dexa significantly increased the enrichment of GR and Pol II at the GRE1 region, while this Dexa-induced enrichment was reduced by treatment with HOG3 (Fig. 5a, lower). At the GRE2 region, Dexa increased Pol II enrichment, which was significantly reduced by both KOG and HOG3. GR enrichment at GRE2 was significantly reduced only by HOG3 treatment (Fig. 5b, lower). Treatment with Dexa also increased the enrichment of FOXO3a and Pol II at the promoters of MuRF-1 and atrogin-1. This increased promoter occupancy was significantly reduced by HOG3 treatment (Fig. 5c and d).

Administration of KOG and HOG3 alleviates skeletal muscle atrophy in rats

To evaluate therapeutic effects of KOG and HOG3 on skeletal muscle atrophy, we established a Dexa-induced skeletal muscle atrophy animal model (Fig. 6a). Since muscles make up 40% of the total weight, we measured changes of body weight for three weeks. The Dexa group of rats with skeletal muscle atrophy showed decreased body weight compared to the Control group of rats with skeletal muscle atrophy. However, administration of

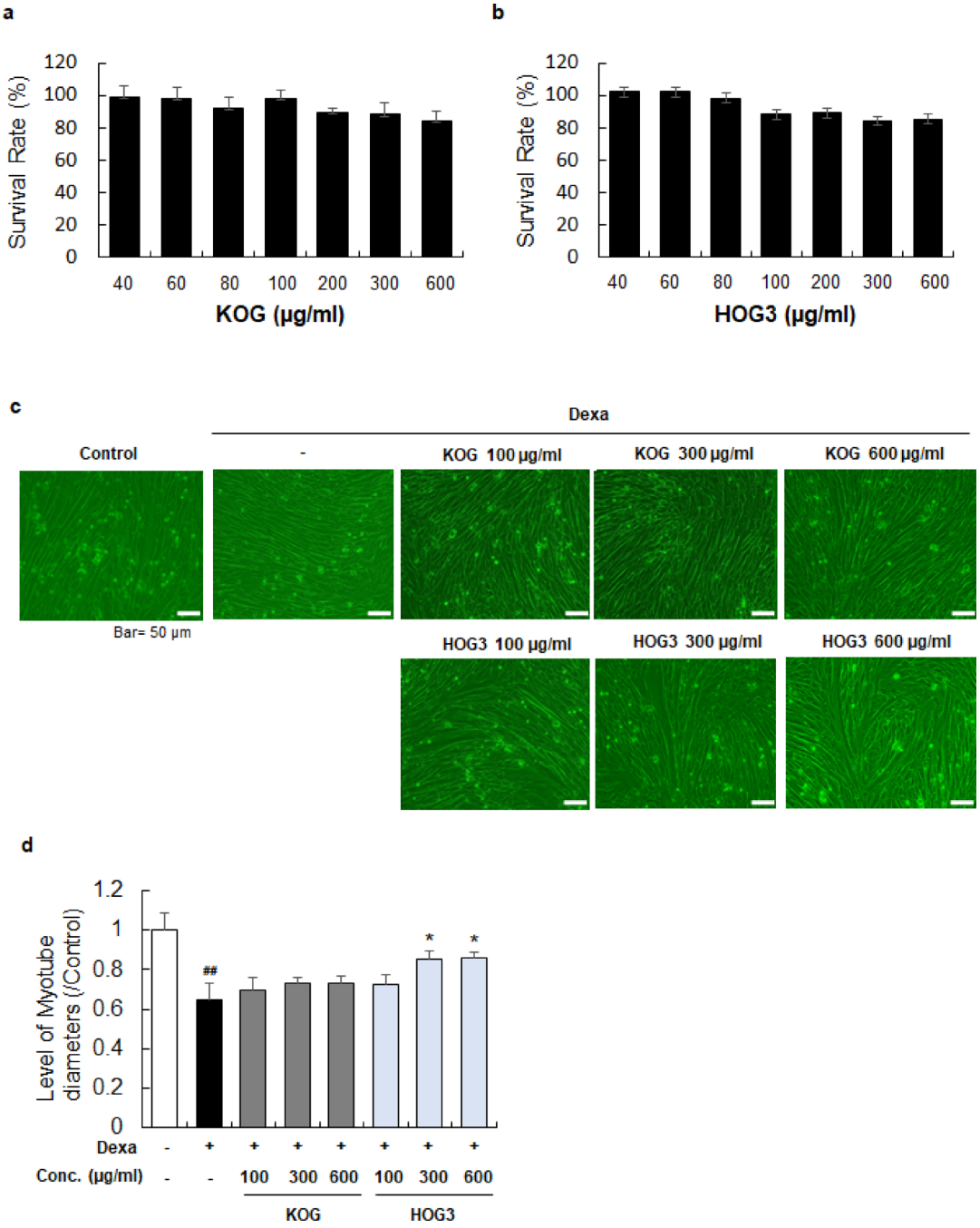

Fig. 3. Effects of KOG and HOG3 treatments on myoblast and myotube cells. (**a** and **b**) Cell viability was determined by MTT assay. L6 cells were cultured with (a) KOG or (b) HOG3 for 24 h. (**c**) Differentiated L6 cells were stimulated with Dexa (dexamethasone, 20 nmol/L, 12 h) and then treated with KOG or HOG3. Myotubes were observed using a microscope. Scale bars = 50 μm. (**d**) Based on representative image, diameters of myotubes were randomly measured in each group using ImageJ. Data are expressed as mean ± SD. Statistical significance is indicated by $^{\#\#}p < 0.01$ compared to the Control group and $^{*}p < 0.05$ compared to the Dexa-only treated group.

HOG3 at 100 or 200 mg/kg significantly suppressed such body weight loss (Fig. 6b). Next, we observed the size of soleus muscle and measured its weight. The Dexa group showed notably reduced size of soleus muscle, whereas KOG and HOG3 increased the size of soleus muscle (Fig. 6c). As shown in Fig. 6d, compared to the Control group, the Dexa group showed significantly reduced weight of soleus muscle. However, administration of KOG or HOG3 inhibited such weight loss of the soleus muscle, especially, the HOG3 group showed significantly recovered weight of the soleus muscle (Fig. 6d). To demonstrate effects of KOG and HOG3 on skeletal muscle atrophy in details, we performed H&E staining and Masson's trichrome staining for soleus muscle and gastrocnemius (Fig. 6e). The Dexa group showed serious damage in muscle bundle, atrophy of muscle fibers

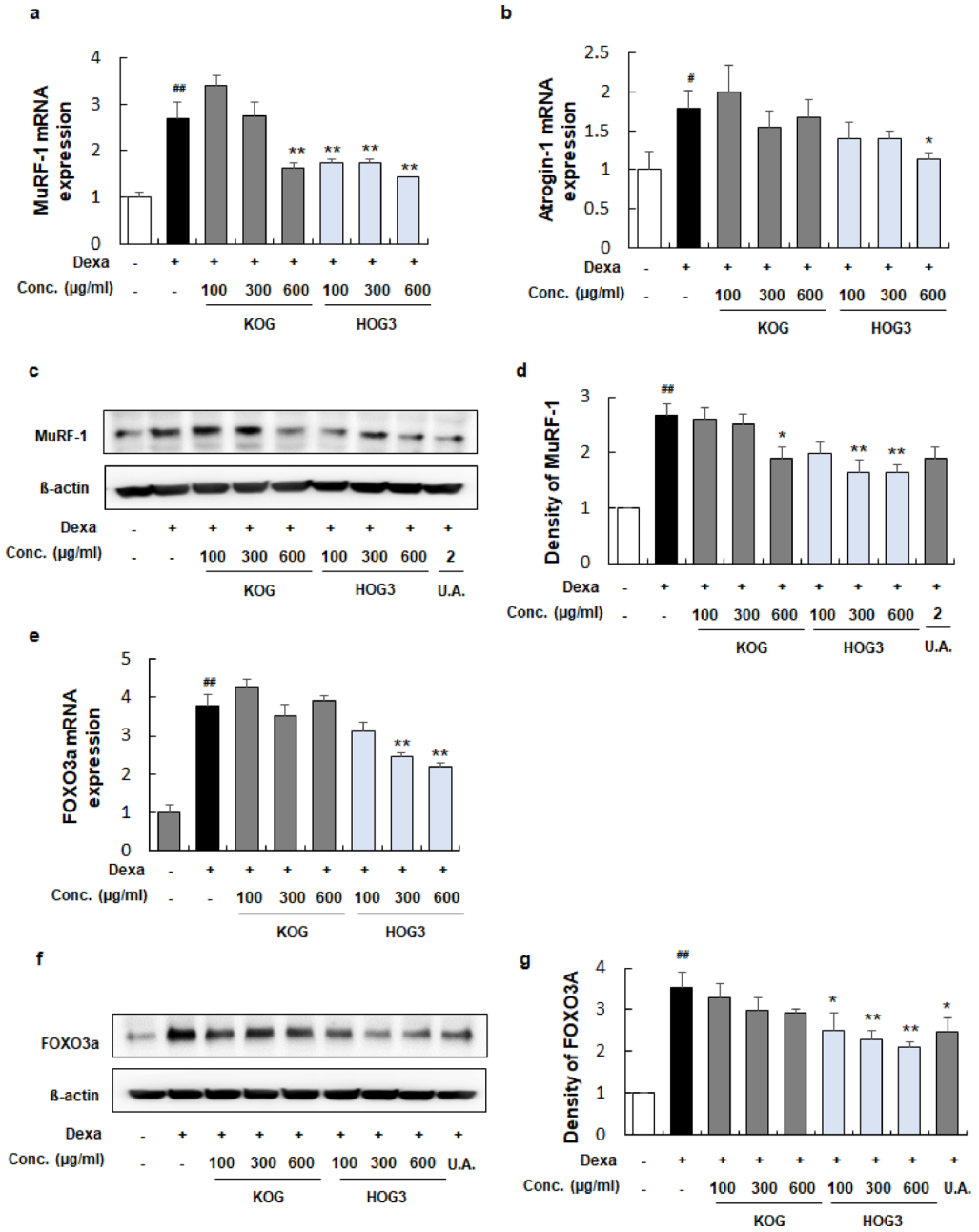

Fig. 4. Inhibitory effects of KOG and HOG3 treatments on MuRF-1, atrogin-1, and FOXO3a in Dexa-stimulated L6 cells. Differentiated L6 cells were stimulated with Dexa to induce muscular atrophy. Dexa-stimulated myotubes were treated with KOG or HOG3. (**a**) mRNA expression of MuRF-1 was determi; ned in Dexa-stimulated myotubes using qRT-PCR. (**b**) mRNA expression of atrogin-1 was determined in Dexa-stimulated myotubes. (**c**) Using Western blotting, protein expression of MuRF-1 was evaluated in Dexa-stimulated myotubes. Ursolic acid was utilized as a positive control. (**d**) Relative protein level of MuRF-1 was normalized by β-actin. (**e**) mRNA expression of FOXO3a in Dexa-stimulated myotubes was quantified. (**f**) Protein level of FOXO3a was detected by western blot assay. (**g**) Relative protein level was measured. $^{\#\#}p < 0.01$, $^{\#}p < 0.05$ vs. the Control group; $^{**}p < 0.01$, $^{*}p < 0.05$ vs. Dexa-only treated group. Kyungohkgo, KOG; HME-processed KOG, HOG3; dexamethasone, Dexa.

(Fig. 6f and h), deposition of collagen (Fig. 6g), and proliferation of connective tissue. However, administration of KOG and HOG3 clearly reduced muscle damage and muscular atrophy and inhibited collagen proliferation. In addition, the inhibitory effect of HOG3 on muscular atrophy was superior to that of KOG (Fig. 6e and h). Administration of HOG3 (200 mg/ml) showed protective potential with significant increased myofiber portion in gastrocnemius muscle (Fig. 6h).

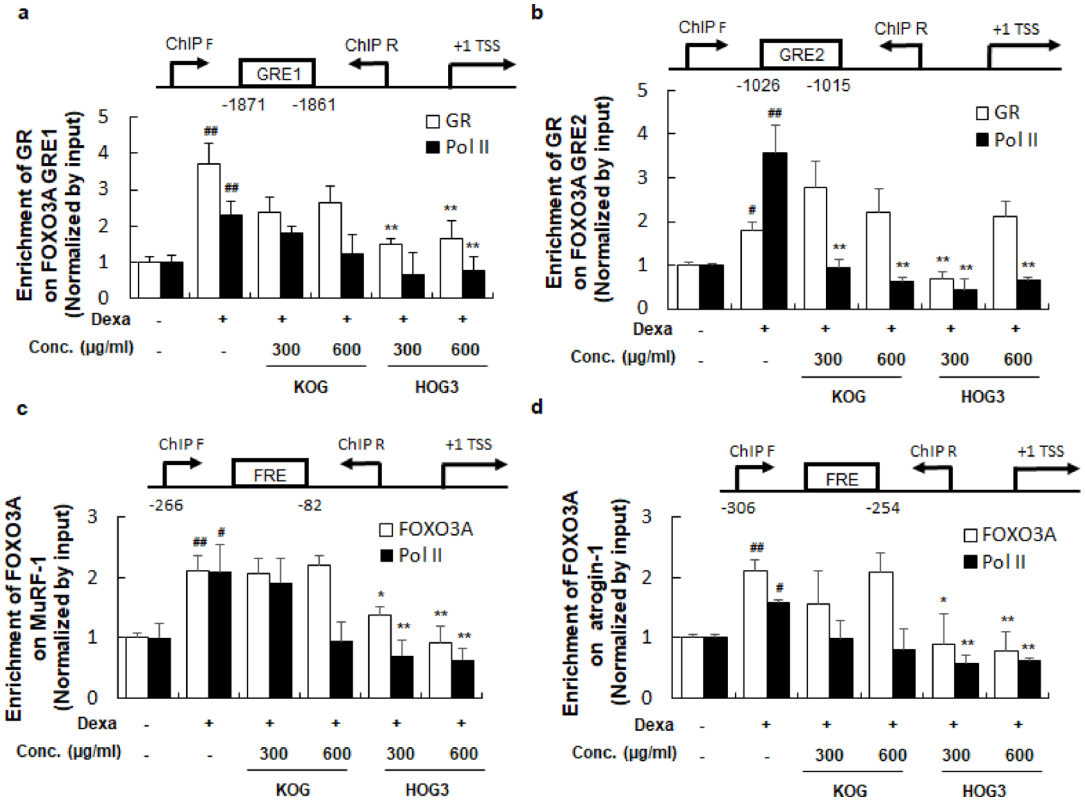

Fig. 5. Effects of KOG and HOG3 treatments on GR, FOXO3a, and Pol II target gene promoters in Dexa-stimulated L6 cells. L6 cells were exposed to Dexa (20 nmol/L) for 16 h, with or without prior treatment with KOG or HOG3. The schematic diagrams illustrate the locations of GC-response elements (GREs) and PCR amplicons within the FOXO3a GRE1 and GRE2 promoters in rats (a, b, upper). Additionally, schematic diagrams depict the positions of the FOXO3a-response element (FRE) and PCR amplicons in the MuRF-1 and atrogin-1 promoters (c, d, upper). Chromatin immunoprecipitation (ChIP) analysis was performed and quantified using qRT-PCR. Dexa treatment led to an increased enrichment of GR, FOXO3a, or Pol II on each promoter, while pretreatment with KOG or HOG3 significantly reduced this enrichment (lower). Statistical significance: $^{\#\#}p < 0.01$, $^{\#}p < 0.05$ vs. the Control group; $^{**}p < 0.01$, $^{*}p < 0.05$ vs. the Dexa-only treated group.

Administration of KOG or HOG3 reduces the expression of MuRF-1, atrogin-1, and FOXO3a in rats with skeletal muscle atrophy

Consistent with the in vitro findings, the expressions of MuRF-1, atrogin-1, and FOXO3a were examined in a Dexa-induced rat model of skeletal muscle atrophy. Dexa treatment significantly increased mRNA expression levels of MuRF-1, atrogin-1, and FOXO3a in rats with skeletal muscle atrophy. In contrast, treatment with KOG (100 and 200 mg/ml) or HOG3 (100 and 200 mg/ml) significantly suppressed mRNA expression of MuRF-1 and atrogin-1. HOG3 at 100 mg/ml only significantly reduced mRNA level of FOXO3a (Fig. 7a and c). The mRNA expression of Follistatin, a negative regulator of myostatin, was significantly increased in the HOG3-treated groups (Fig. 7d). Next, we analyzed ALP level. Positive staining of ALP is associated with abnormal fiber in muscles. Dexa treatment increased the level of ALP, whereas HOG3 at 200 mg/ml significantly decreased ALP levels in rats with skeletal muscle atrophy (Fig. 7e).

Discussion

Compared with single-screw systems, twin-screw HME provides superior distributive and dispersive mixing, enabling the production of highly homogeneous dispersions. During HME, the active pharmaceutical ingredients, thermoplastic carriers, and excipients are heated and softened within the barrel and subsequently forced through a die to form homogeneous granules. This melt processing approach promotes molecular-level mixing and yields extrudates with excellent content uniformity and batch-to-batch consistency. As with other pharmaceutical dosage forms, a broad range of excipients — including antioxidants, thermal lubricants, processing aids, matrix carriers, release modifiers, and bulking agents—can be incorporated to optimize manufacturability and functional performance[23,24]. Among these, plasticizers play a particularly important role by reducing processing temperature, minimizing thermal or shear-induced degradation, and regulating softening and fusion behavior. In this study, ascorbic acid served as a plasticizing antioxidant and contributed to the stabilization of thermolabile constituents during extrusion. One limitation of this study is related to the formulation of HOG3, specifically the inclusion of ascorbic acid and ascorbyl palmitate. These compounds were incorporated primarily as essential stabilizers to prevent thermal degradation and oxidative damage to active

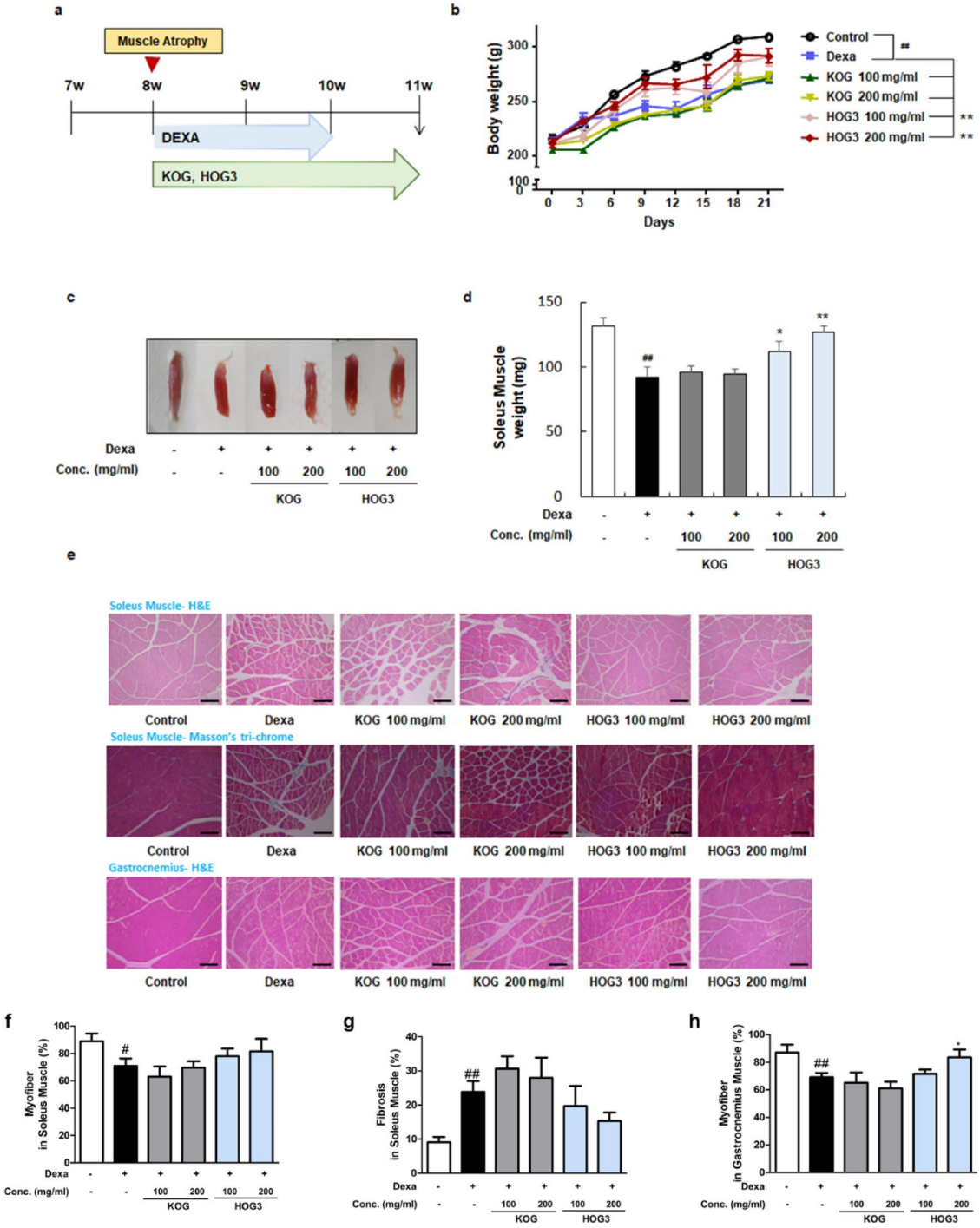

Fig. 6. Protective effects of KOG and HOG3 administration in rats with skeletal muscle atrophy. (**a**) Scheme of Dexa-induced skeletal muscle atrophy animal model. (**b**) Body weight was measured every three days. (**c**) Representative image of soleus muscle from each experimental group. (**d**) Weight of soleus muscle was measured for each experimental group. All results are presented as mean ± SD. $^{\#\#}p < 0.01$ vs. the Control group; $^{**}p < 0.01$, $^{*}p < 0.05$ vs. the Dexa group. (**e**) Soleus muscle and gastrocnemius muscle were stained with H&E and Masson's trichrome. The quantitative analyses were measured with (**e**): myofiber portion in soleus muscle (**f**), fibrosis area in soleus muscle (**g**), and myofiber portion in gastrocnemius muscle (**h**). Kyungohkgo, KOG; HME-processed KOG, HOG3; dexamethasone, Dexa.

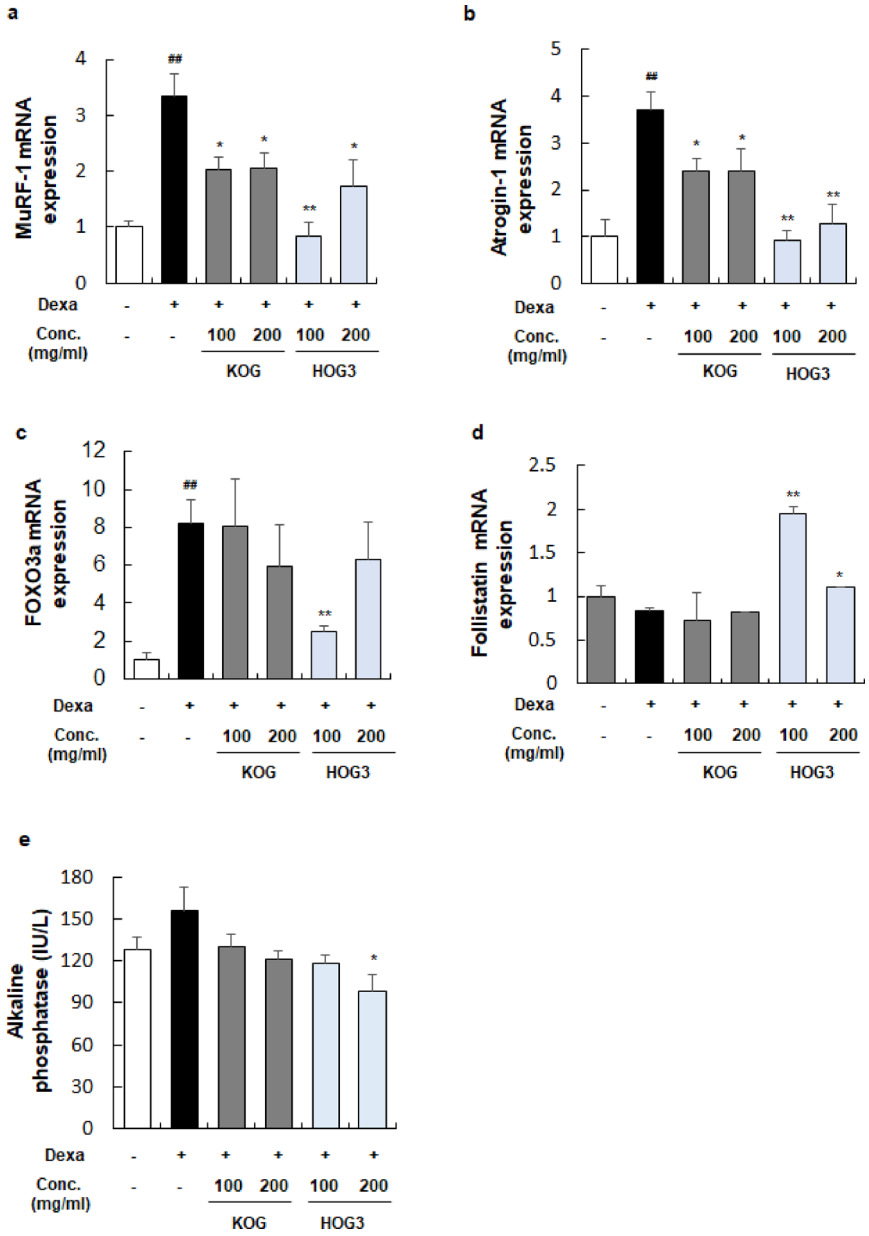

Fig. 7. Regulatory effects of KOG and HOG3 administration on MuRF-1/atrogin-1/FOXO3a signaling in rats with skeletal muscle atrophy. (**a**–**d**) mRNA levels of (a) MuRF-1, (b) atrogin-1, (c) FOXO3a and (d) Follistatin were determined using qRT-PCR and quantified. (**e**) The level of alkaline phosphatase (ALP) was measured using serum samples from rats. Kyungohkgo, KOG; HME-processed KOG, HOG3.

ingredients during the high-temperature HME processing. While their inclusion was necessary to ensure the physicochemical stability and quality of the final product, we acknowledge that their intrinsic antioxidant and cytoprotective activities[25] may present a confounding factor.

Accordingly, the anti-atrophic effects observed in this study should be interpreted as the collective efficacy of the optimized final formulation, potentially arising from synergistic interactions between HME-enhanced minor ginsenosides and bioactive excipients. Although the analytically significant increase in minor ginsenoside content in HOG3 strongly suggests HME-driven chemical transformation, the specific biological contribution of the excipients was not isolated in the current experimental design. To definitively distinguish the pharmacological actions of the herbal constituents from those of the excipients, future studies will incorporate rigorous controls, including HME-processed excipient-only vehicles, to clarify their respective roles.

Among consists of KOG, four medicinal herbs, each containing bioactive compounds with established relevance to skeletal muscle protection. *P. ginseng*, primarily through its ginsenoside constituents, has been presented to alleviate muscle atrophy by suppressing the FOXO3a-MuRF-1-atrogin-1 signaling pathway[28,29], and ginsenoside Rg3 has demonstrated direct anti-atrophic effects in vitro[30]. *R. glutinosa*, the primary component of KOG, has shown protective effects against muscle loss in osteoporotic and diabetic models, partly through

inhibition of FOXO1-dependent ubiquitin-proteasome results[32,33]. *P. cocos* contains beta-glucans with anti-inflammatory effects and anti-oxidative activity, which may contribute to preservation of myofiber integrity under catabolic conditions[34]. Honey, bee-biproduct, and its derived components have also been reported to modulate myoblast and myocyte function[35]. Collectively, these findings suggest that the multi-component composition of KOG may exert complementary and convergent downstream effects on atrophy-associated gene expression, particularly within FOXO-dependent protein degradation pathways.

Based on previous studies, KOG and its HME-processed formulation, HOG3, seem to be promising therapeutic candidates for skeletal muscle atrophy. Network pharmacological analyses supported mechanistic links between KOG and muscle atrophy-related targets, including FoxO, atrogin-1 (FBXO32), or MuRF-1 (TRIM63) (Fig. 1). These results positioned FOXO signaling sits at the core of sarcopenia-related molecular networks, integrating upstream regulators such as AMPK, Akt, and MAPK with downstream effectors including atrogin-1 and MuRF-1. The analysis propounded that traditional oriental medicine, KOG, may exert protective effects by modulating these interconnected signaling networks as well as suppressing FOXO-driven catabolic gene expression, thereby justifying further experimental investigation of HOG3 in sarcopenic models.

Up to now, Dexa administration has been widely used to establish experimental models of sarcopenia and skeletal muscle atrophy. Injection of Dexa can induce muscle degeneration in young rats and cause weight loss in young rodents. However, this phenotype does not fully recapitulate the clinical observation that a substantial proportion of older individuals with muscle atrophy exhibit increased body weight. Nevertheless, Dexa-induced muscle atrophy models offer significant advantages for studying imbalance between protein synthesis and degradation in skeletal muscle. Additionally, previous studies have reported that excess Dexa exposure can induce pronounced muscle wasting by disrupting the balance between contractile proteins synthesis and degradation.

Under muscle atrophic conditions, disruption of the equilibrium between protein synthesis and degradation result in progressive muscle mass loss and functional impairment . Proteolysis of myofibrillar proteins is primarily mediated by the ubiquitin-proteasome system, and muscle weakness reflects deterioration of the contractile apparatus. The two muscle-specific E3 ubiquitin ligases, MuRF-1 and atrogin-1, are consistently upregulated across diverse forms of muscle wasting making them robust prominent biomarkers of skeletal muscle atrophy. Transcription factor FOXO3a is a well-established regulator of both atrogin-1 and MuRF-1. In this study, Dexa-induced increases in FOXO3a expression and promoter occupancy were consistently attenuated by HOG3 treatment, supporting a mechanistic relationship between HOG3 treatment and suppression of FOXO-dependent transcriptional programs.

FoxO transcription factors can bind to the FOXO-responsive elements within the proximal promoter of atrogin-1 and MuRF-1 to drive the transcription. Previous study has demonstrated that Dexa significantly enhanced FoxO-driven MuRF-1 promoter activity, indicating that FoxO may require cooperative DNA-binding partners for maximal transcriptional activation. In Fig. 1, network analyses further illustrated interactions among FOXO, TRIM63 or FBXO32 muscle atrophy biomarkers and KOG, while also revealing additional signaling pathways through which KOG may influence muscle homeostasis, metabolism, and apoptosis.

In this study, HOG3 was prepared by applying HME to KOG, yielding nanoscale particles as confirmed by TEM and particle-size analysis (Fig. 2a- c). Nanosizing increases specific surface area and wettability, thereby accelerating dissolution and enhancing apparent aqueous concentration of active constituents. In parallel, HME frequently converts crystalline actives into amorphous solid dispersions, a solid-state transition known to improve apparent solubility and oral absorption. Consistent with prior work, HME processing has been shown to increase the aqueous solubility/dispersibility of botanical actives with such improvements correlating with increased in vivo exposure and pharmacodynamic efficacy. Therefore, these findings support HME as an enabling technology for KOG, whereby nanosizing and amorphization jointly yield a bio-pharmaceutically superior formulation (HOG3) suitable for oral intervention in skeletal muscle atrophy.

We investigated the pharmacological effects of KOG and HOG3 on skeletal muscle atrophy using both in vivo and in vitro models. Treatment with KOG or HOG3 promoted myoblast differentiation in Dexa-induced L6 cells through regulation of MuRF-1, atrogin-1, and FOXO3a (Figs. 3 and 4). Notably, HOG3 presented stronger inhibitory effects on MuRF-1 and FOXO3a protein expression than UA, a compound known to confer resistance exercise-like benefits on muscle mass. Additionally, HOG3 significantly inhibited the promoter activities of FOXO3a, MuRF-1, and atrogin-1 (Fig. 5), demonstrating that HOG3 more effectively reduced the expression and promoter occupancy of FOXO3a, MuRF-1, and atrogin-1 compared with KOG under Dexa-induced atrophic conditions.

Animal study demonstrated that administration of HOG3 significantly restored body weight and muscle mass in Dexa-induced atrophic animals (Fig. 6a- d). During skeletal muscle degeneration, excessive fibroblasts and extracellular matrix components can replace resident muscle fibers, resulting in a reduction in muscle mass. HOG3 administration suppressed serious damage in muscle bundle and inhibited deposition of collagen, suggesting a therapeutic protective effect of HOG3 against structural muscle deterioration (Fig. 6e). Consistent with in vitro experiment, administration with KOG or HOG3 inhibited the expression of MuRF-1, atrogin-1, and FOXO3a in atrophic muscle tissue (Fig. 7a- c). Meanwhile, HOG3 modulated follistatin and alkaline phosphatase levels, hinting partial recovery effects of HOG3 on abnormal muscle physiology.

Despite these findings, upstream regulatory mechanisms remain incompletely defined. Although KOG and HOG3 clearly modulated FOXO-dependent catabolic gene expression, their precise positioning within the GC-Akt-FOXO3a signaling axis has not been fully elucidated. Given that FOXO3a activity is primarily regulated through Akt-mediated phosphorylation, direct assessment of phosphorylated FOXO3a would strengthen mechanistic interpretation. Since FOXO3a activity is predominantly governed by Akt-mediated phosphorylation, direct evaluation of p-FOXO3a would strengthen the mechanistic linkages between glucocorticoid signaling, FOXO3a activation, and E3 ubiquitin ligase expression[54]. Dexa-induced muscle atrophy is initiated by GR

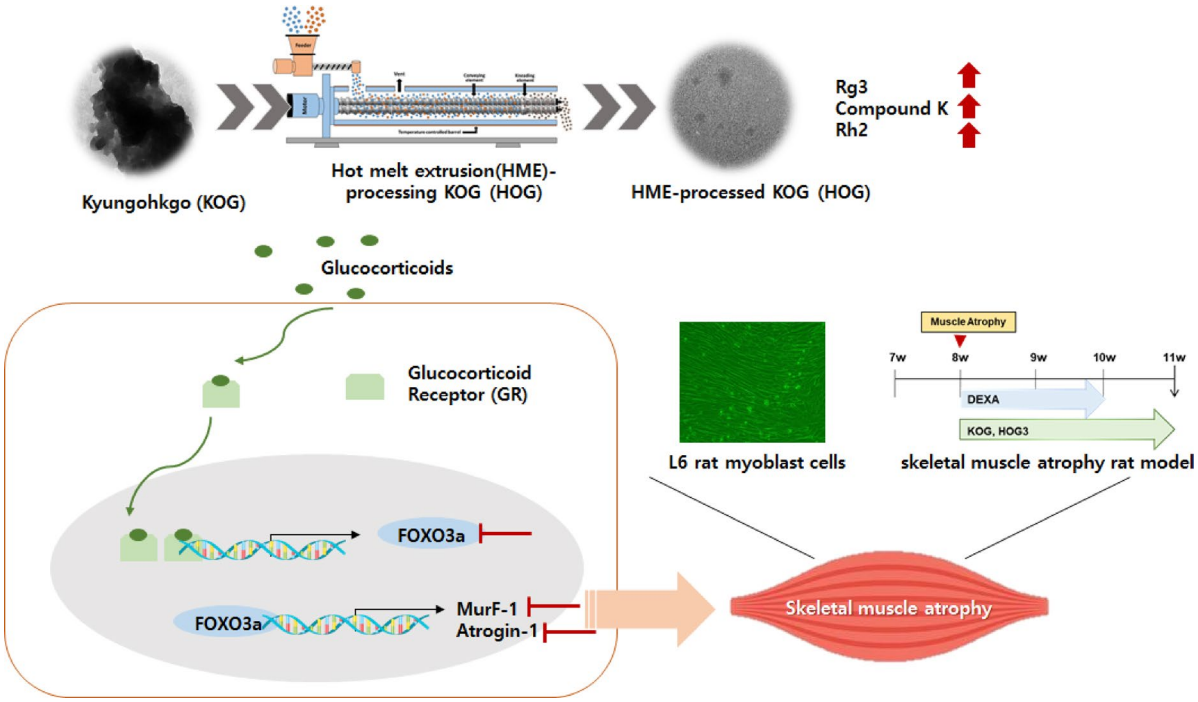

Fig. 8. Schematic representation of the effects of KOG or HOG3 on dexamethasone-induced skeletal muscle atrophy. This figure illustrates the proposed mechanisms by which KOG or HOG3 attenuates muscle atrophy by downregulating the FOXO3a/MuRF-1/atrogin-1 axis.

activation; therefore, HOG3 may act through multiple upstream mechanisms, including attenuation of GR signaling, inhibition of FOXO3a nuclear translocation, or enhancement of FOXO3a inactivation via altered phosphorylation or degradation dynamics. While our findings indicate that KOG and HOG3 affect important pathways related to muscle protein catabolism, their precise positioning within the GC-Akt-FOXO3a axis[55] has not been fully delineated. Even though the findings showed the suppressive effects on major atrophy-associated markers, precise upstream inhibitory results still remained undetermined. The present design focused on the downstream regulating FOXO-dependent protein degradation pathways. Therefore, it is not distinguishable leaving various possibilities of those upstream. To clarify the involvement of HOG3 on GR signaling, the Akt-FOXO3a phosphorylation axis or FOXO3a stability would be required for additional studies. Future studies incorporating phosphorylation-level analyses and GR signaling assessments will be required to clarify the precise molecular mechanisms underlying the anti-atrophic effects of HOG3.

Conclusions

Findings of this study indicate that KOG and its HME-formulation, HOG3, present beneficial effects against skeletal muscle atrophy in both in vivo and in vitro models. KOG has long been used as one of the tonic formula composed of four herbal medicines: *P. ginseng*, *R. glutinosa*, *P. cocos*, and honey. Each of them contains bioactive constituents previously associated with muscle-protective effects. In the present study, HME processing enhanced the aqueous dispersibility and bioavailability of KOG, resulting in the optimized formulation HOG3. Treatment with HOG3 consistently reduced the expression and promoter occupancy of key atrophy-associated markers, including FOXO3a, MuRF-1, and atrogin-1, under glucocorticoid-induced atrophic conditions. These results were observed in both Dexa-stimulated L6 myotubes and a rat model of skeletal muscle atrophy. Although the precise upstream mechanism regulating FOXO3a activity was not directly analyzed, the results would support that HOG3 attenuates FOXO-dependent catabolic gene expression as a downstream response to glucocorticoid stimulation. As a result, these findings suggest its pharmacological potential and that HOG3 represents a promising candidate for further development as a therapeutic approach for preventing or ameliorating skeletal muscle atrophy (Fig. 8).

Data availability

Data will be made available on request to Yun-Yeop Cha, one of the corresponding authors.

Received: 16 September 2025; Accepted: 6 March 2026
Published online: 19 March 2026

References

1. Baskin, K. K., Winders, B. R. & Olson, E. N. Muscle as a mediator of systemic metabolism. *Cell. Metab.* **21**, 237–248. https://doi.org/10.1016/j.cmet.2014.12.021 (2015).
2. Fanzani, A., Conraads, V. M., Penna, F. & Martinet, W. Molecular and cellular mechanisms of skeletal muscle atrophy: An update. *J. cachexia sarcopenia muscle*. **3**, 163–179. https://doi.org/10.1007/s13539-012-0074-6 (2012).
3. Wilkinson, D. J., Piasecki, M. & Atherton, P. J. The age-related loss of skeletal muscle mass and function: Measurement and physiology of muscle fibre atrophy and muscle fibre loss in humans. *Ageing Res. Rev.* **47**, 123–132. https://doi.org/10.1016/j.arr.2018.07.005 (2018).
4. Souza, V. A. et al. Sarcopenia in patients with chronic kidney disease not yet on dialysis: Analysis of the prevalence and associated factors. *PloS one*. **12**, e0176230. https://doi.org/10.1371/journal.pone.0176230 (2017).
5. Goates, S. et al. Economic Impact of Hospitalizations in US Adults with Sarcopenia. *J. frailty aging*. **8**, 93–99. https://doi.org/10.14283/jfa.2019.10 (2019).
6. Bruyere, O., Beaudart, C., Ethgen, O., Reginster, J. Y. & Locquet, M. The health economics burden of sarcopenia: A systematic review. *Maturitas* **119**, 61–69. https://doi.org/10.1016/j.maturitas.2018.11.003 (2019).
7. Xie, W. Q. et al. Mouse models of sarcopenia: Classification and evaluation. *J. cachexia sarcopenia muscle*. **12**, 538–554. https://doi.org/10.1002/jcsm.12709 (2021).
8. Permpoon, U., Moon, J., Kim, C. Y. & Nam, T. G. Glucocorticoid-mediated skeletal muscle atrophy: Molecular mechanisms and potential therapeutic targets. *Int. J. Mol. Sci.* **26** (15), 7616. https://doi.org/10.3390/ijms26157616 (2025).
9. Webster, J. M., Fenton, C. G., Langen, R. & Hardy, R. S. Exploring the Interface between Inflammatory and Therapeutic Glucocorticoid Induced Bone and Muscle Loss. *Int. J. Mol. Sci.* **20** https://doi.org/10.3390/ijms20225768 (2019).
10. Surmachevska, N. & Tiwari, V. in *StatPearls* (2023).
11. Shen, S. et al. Myricanol rescues dexamethasone-induced muscle dysfunction via a sirtuin 1-dependent mechanism. *J. cachexia sarcopenia muscle*. **10**, 429–444. https://doi.org/10.1002/jcsm.12393 (2019).
12. Kohn, J. A., Deshpande, K. & Ortlund, E. A. Deciphering modern glucocorticoid cross-pharmacology using ancestral corticosteroid receptors. *J. Biol. Chem.* **287**, 16267–16275. https://doi.org/10.1074/jbc.M112.346411 (2012).
13. Kuo, T., Harris, C. A. & Wang, J. C. Metabolic functions of glucocorticoid receptor in skeletal muscle. *Mol. Cell. Endocrinol.* **380**, 79–88. https://doi.org/10.1016/j.mce.2013.03.003 (2013).
14. Castillero, E., Alamdari, N., Lecker, S. H. & Hasselgren, P. O. Suppression of atrogin-1 and MuRF1 prevents dexamethasone-induced atrophy of cultured myotubes. *Metab. Clin. Exp.* **62** (10). https://doi.org/10.1016/j.metabol.2013.05.018 (2013).
15. Penniman, Christie, M. et al. Loss of FoxOs in muscle increases strength and mitochondrial function during aging. *J. cachexia sarcopenia muscle*. **14** https://doi.org/10.1002/jcsm.13124 (2023).
16. Chen, F. et al. Potential adverse effects of Dexamethasone therapy on COVID-19 patients: Review and recommendations. *Infect. Dis. therapy*. **10**, 1907–1931. https://doi.org/10.1007/s40121-021-00500-z (2021).
17. Hwang, D. S. et al. Effect of a Traditional Herbal Prescription, Kyung-Ok-Ko, on Male Mouse Spermatogenic Ability after Heat-Induced Damage. *Evidence-based Complement. Altern. medicine: eCAM vol.* **950829** https://doi.org/10.1155/2015/950829 (2015).
18. Choi, J. H., Jang, M., Lee, J. I., Chung, W. S. & Cho, I. H. Neuroprotective Effects of a Traditional Multi-Herbal Medicine Kyung-Ok-Ko in an Animal Model of Parkinson's Disease: Inhibition of MAPKs and NF-kappaB Pathways and Activation of Keap1-Nrf2 Pathway. *Front. Pharmacol.* **9** https://doi.org/10.3389/fphar.2018.01444 (2018).
19. Kim, K. I., Kong, M., Lee, S. H. & Lee, B. J. The efficacy and safety of Kyung-Ok-Ko on cancer-related fatigue in lung cancer patients: Study protocol for a randomized, patients-assessor blind, placebo-controlled, parallel-group, single-center trial. *Medicine* **98**, e17717. https://doi.org/10.1097/MD.0000000000017717 (2019).
20. Ren, Y., Mei, L., Zhou, L. & Guo, G. Recent perspectives in hot melt extrusion-based polymeric formulations for drug delivery: Applications and innovations. *Aaps Pharmscitech*. **20**, 92 (2019).
21. Kanehisa, M. & Goto, S. KEGG: Kyoto encyclopedia of genes and genomes. *Nucleic Acids Res.* **28**, 27–30. https://doi.org/10.1093/nar/28.1.27 (2000).
22. Kanehisa, M., Sato, Y., Kawashima, M., Furumichi, M. & Tanabe, M. KEGG as a reference resource for gene and protein annotation. *Nucleic Acids Res.* **44**, D457–462. https://doi.org/10.1093/nar/gkv1070 (2016).
23. Seok, Y. M. et al. Mountain ginseng inhibits skeletal muscle atrophy by decreasing muscle RING finger protein-1 and atrogin1 through forkhead box O3 in L6 myotubes. *J. Ethnopharmacol.* **270**, 113557 (2021).
24. Ke, Y. et al. Preparation and pharmacological effects of minor ginsenoside nanoparticles: A review. *Front. Pharmacol.* **13**, 974274 (2022).
25. Azad, M. O. K. et al. Development of a polymer-mediated soybean nanocomposite by hot melt extrusion to improve its functionality and antioxidant properties. *Foods* **8**, 41 (2019).
26. Censi, R., Gigliobianco, M. R., Casadidio, C. & Di Martino, P. Hot Melt Extrusion: Highlighting Physicochemical Factors to Be Investigated While Designing and Optimizing a Hot Melt Extrusion Process. *Pharmaceutics* **10**, 89 (2018).
27. Crowley, M. M. et al. Pharmaceutical Applications of Hot-Melt Extrusion: Part I. *Drug Dev. Ind. Pharm.* **33**, 909–926. https://doi.org/10.1080/03639040701498759 (2007).
28. Kim, H. S. et al. Effect of red ginseng on genotoxicity and health-related quality of life after adjuvant chemotherapy in patients with epithelial ovarian cancer: A randomized, double blind, placebo-controlled trial. *Nutrients* **9**, 772 (2017).
29. Wan, Y. et al. Panax ginseng and its ginsenosides: Potential candidates for the prevention and treatment of chemotherapy-induced side effects. *J. Ginseng Res.* **45**, 617–630 (2021).
30. Kim, R., Kim, J. W., Lee, S. J. & Bae, G. U. Ginsenoside Rg3 protects glucocorticoid–induced muscle atrophy in vitro through improving mitochondrial biogenesis and myotube growth. *Mol. Med. Rep.* **25**, 1–9 (2022).
31. Zhang, R. X., Li, M. X. & Jia, Z. P. Rehmannia glutinosa: Review of botany, chemistry and pharmacology. *J. Ethnopharmacol.* **117**, 199–214 (2008).
32. Ou, L. et al. Effects of Rehmannia glutinosa polysaccharides on bone tissue structure and skeletal muscle atrophy in rats with disuse. *Acta cirurgica brasileira* 36 (2021).
33. Tseng, Y. T. et al. Protective effects of Liuwei dihuang water extracts on diabetic muscle atrophy. *Phytomedicine* **53**, 96–106 (2019).
34. Nie, A. et al. Phytochemistry and pharmacological activities of Wolfiporia cocos (FA Wolf) Ryvarden & Gilb. *Front. Pharmacol.* **11**, 505249 (2020).
35. Ali, A. M. & Kunugi, H. Apitherapy for age-related skeletal muscle dysfunction (sarcopenia): A review on the effects of royal jelly, propolis, and bee pollen. *Foods* **9**, 1362 (2020).
36. Kaasik, P. et al. Ageing and dexamethasone associated sarcopenia: Peculiarities of regeneration. *J. Steroid Biochem. Mol. Biol.* **105**, 85–90 (2007).
37. Cao, R. Y., Li, J., Dai, Q., Li, Q. & Yang, J. Muscle atrophy: Present and future. *Muscle atrophy*, 605–624 (2018).
38. Singh, A., PHOG3at, J., Yadav, A. & Dabur, R. The dependency of autophagy and ubiquitin proteasome system during skeletal muscle atrophy. *Biophys. Rev.* **13**, 203–219 (2021).
39. Bodine, S. C. & Baehr, L. M. Skeletal muscle atrophy and the E3 ubiquitin ligases MuRF1 and MAFbx/atrogin-1. *Am. J. Physiology-Endocrinology Metabolism*. **307**, E469–E484 (2014).
40. Ridhurkar, D., Vajdai, A. & Zsigmond, Z. Hot-melt extrusion (HME) and its application for pharmacokinetic improvement of poorly water soluble drugs. *Pharmacology Toxicol. Biomedical Reports* **2** (2016).

41. Giri, B. R. et al. Hot-Melt Extruded Amorphous Solid Dispersion for Solubility, Stability, and Bioavailability Enhancement of Telmisartan. *Pharmaceuticals (Basel)*. 14. https://doi.org/10.3390/ph14010073 (2021).
42. Jadhav, P., Gokarna, V., Deshpande, V. & Vavia, P. Bioavailability Enhancement of Olmesartan Medoxomil Using Hot-Melt Extrusion: In-Silico, In-Vitro, and In-Vivo Evaluation. *AAPS PharmSciTech*. **21**, 254. https://doi.org/10.1208/s12249-020-01780-3 (2020).
43. Lee, J., Lee, H. Y. & Baek, J. S. Enhanced Minor Ginsenoside Contents of Nano-Sized Black Korean Ginseng through Hot Melt Extrusion. *Mater. (Basel)*. **17** https://doi.org/10.3390/ma17184612 (2024).
44. Ryu, S., Lee, H. Y., Nam, S. H. & Baek, J. S. Antifungal Activity of Angelica gigas with Enhanced Water Solubility of Decursin and Decursinol Angelate by Hot-Melt Extrusion Technology against Candida albicans. *Int. J. Translational Med.* **2**, 515–521 (2022).
45. Kim, H. B., Ryu, S. & Baek, J. S. The Effect of Hot-Melt Extrusion of Mulberry Leaf on the Number of Active Compounds and Antioxidant Activity. *Plants (Basel)*. **11** https://doi.org/10.3390/plants11223019 (2022).
46. Zhao, Y., Xu, X., Dai, A., Jia, Y. & Wang, W. Enhanced Dissolution and Bioavailability of Curcumin Nanocrystals Prepared by Hot Melt Extrusion Technology. *Int. J. Nanomed.* **19**, 5721–5737. https://doi.org/10.2147/IJN.S463918 (2024).
47. Go, E. J. et al. Regulation of Intestinal Barrier Function and Gut Microbiota by Hot Melt Extrusion-Drug Delivery System-Prepared Mulberry Anthocyanin in an Inflammatory Bowel Disease Model. *Pharmaceuticals (Basel)*. **18** https://doi.org/10.3390/ph18040475 (2025).
48. Kang, Y. S., Noh, E. B. & Kim, S. H. Effects of ursolic acid on muscle mass and bone microstructure in rats with casting-induced muscle atrophy. *J. Exerc. Nutr. Biochem.* **23**, 45 (2019).
49. Chen, H. et al. Silencing COX-2 blocks PDK1/TRAF4-induced AKT activation to inhibit fibrogenesis during skeletal muscle atrophy. *Redox Biol.* **38**, 101774 (2021).
50. Zha, W. et al. Ginseng and ginsenosides: Therapeutic potential for sarcopenia. *Biomedicine & pharmacotherapy = Biomedecine & pharmacotherapie* vol. 156. (2022). https://doi.org/10.1016/j.biopha.2022.113876
51. Won, H. J. et al. Non-clinical pharmacokinetic behavior of ginsenosides. *J. ginseng Res.* **43** https://doi.org/10.1016/j.jgr.2018.06.001 (2019).
52. Wang, H. et al. Ginsenosides emerging as both bifunctional drugs and nanocarriers for enhanced antitumor therapies. *J. Nanobiotechnol.* **19** https://doi.org/10.1186/s12951-021-01062-5 (2021).
53. Arring, Noël, M. et al. Ginseng as a Treatment for Fatigue: A Systematic Review. *J. Altern. Complement. Med. (New York N Y)*. https://doi.org/10.1089/acm.2017.0361 (2018).
54. Zheng, B. et al. FOXO3a mediates signaling crosstalk that coordinates ubiquitin and atrogin-1/MAFbx expression during glucocorticoid-induced skeletal muscle atrophy. *FASEB journal: official publication Federation Am. Soc. Experimental Biology*. **24** https://doi.org/10.1096/fj.09-151480 (2010).
55. Liu, Q. et al. Identification of a novel small-molecule inhibitor of miR-29b attenuates muscle atrophy. *Mol. therapy Nucleic acids*. **31** https://doi.org/10.1016/j.omtn.2023.02.003 (2023).

Author contributions

Y.M.S., B.R.J., J.S.B., Y.Y.C. and H.J.A. conceived and designed the experiments; Y.M.S, S.R., C.Y.J., Y.J. and J.S. performed the experiments; Y.M.S., B.R.J., T.Y.G., M.S.S., J.S.B and H.J.A. analyzed the data; J.S.B and H.J.A. provided the reagents, materials, and analysis tools; B.R.J., Y.Y.C., J.S.B, and H.J.A. drafted the manuscript. S.R., T.Y.G., H.J.A., J.S.B., and Y.Y.C. revise the article. All authors read and approved the final manuscript.

Funding

This research was supported by a grant of the National Institute for Korean Medicine Development (NIKOM) ⌜Korean medicine industry advancement support project⌟ funded by the Daegu Metropolitan City, the Province of Gyeongsangbuk-do, the Ministry of Health and Welfare, Republic of Korea (3234 – 302).This research was supported by a grant of the Korea Health Technology R&D Project through the National Research Foundation (NRF) & the Korea Health Industry Development Institute (KHIDI), funded by the Ministry of Science and ICT, Republic of Korea & the Ministry of Health & Welfare, Republic of Korea (No. RS-2023-00262645).

Declarations

Competing interests

The authors declare no competing interests.

Additional information

Supplementary Information The online version contains supplementary material available at https://doi.org/10.1038/s41598-026-43874-1.

Correspondence and requests for materials should be addressed to H.-J.A., J.-S.B. or Y.-Y.C.